

# **A Wide Speed Operation of SRM Using Low Cost Encoder and Controller**

Young Jim Lee<sup>1</sup>, Sung Jun Park<sup>2</sup>, Han Woong Park<sup>3</sup> and Man Hyung Lee<sup>4</sup>

<sup>1</sup> Dept. of Intelligent Mechanical System Engineering, Pusan National University, Pusan, Korea

<sup>2</sup> Dept. of Electrical Engineering, Tongmyong College, Pusan, Korea

<sup>3</sup> Dept. of Electrical Engineering, Korea Naval Academy, Jinhae, KyungNam, Korea

<sup>4</sup> School of Mech. Eng. & ERC/Net Shape and Die Manufacturing, Pusan National University, Pusan, Korea

## **ABSTRACT**

In switched reluctance motor (SRM) drives, the turn-on and turn-off angles of each phase switch should be accurately controlled for accuracy and efficiency. The accuracy of the switching angles is mainly dependent upon the resolution of the encoder and the sampling period of the microprocessor, that are used to provide the information of the rotor position and to implement a control algorithm of the SRM, respectively. Thus, the higher the speed of the SRM is increased, the larger the amount of the switching angle deviations are from the preset turn-on and turn-off angles. Consequently, the motor can not be driven stably in high speed region. Therefore, a simple and low cost encoder suitable for the practical and stable SRM drive is proposed and the control algorithm to provide the switching signals using a simple digital logic circuit is also presented for a wide speed range operation

**Keywords** · SRM, Encoder, high speed operation, high precision angle control

## **1. Introduction**

The SRM(Switched Reluctance Motor) is a simple, low-cost robust motor suitable for variable-speed as well as servo-type applications. With relatively simple converter and control requirements, the SRM is gaining attention from the drive industry. However, high torque ripple generated by the motor during the commutation periods, acoustic noise, expensive position sensing requirements, and lack of suitable converters for low-voltage applications are limiting the SRM from becoming the core of the modern motor drive industry

Control of the SRM can be done in different ways. Basically, there exist three different control methods : voltage control, current control, and single pulse control [1]. The current control method is normally used to control the torque efficiently, while single pulse method is used for high-speed operation. Voltage control has no limitation of the current as the current sensor is not required, which makes it applicable in low-cost systems.

Due to the development of micro-controllers, the control loops have changed from analog to digital implementation, which allows more advanced control features. Also, achieving optimal excitation for the SRM drive is becoming a major requirement in various high power applications. The various optimal control strategies could be to obtain maximum torque per ampere, maximum efficiency, etc.

However, whatever the control methods are adopted, it is essential to synchronize the stator phase excitation with the rotor position. In addition, to enhance the SRM drive's torque-speed capability and efficiency, the turn-on and turn-off angles must be carefully scheduled with speed, and the duration of the commutation period becomes more important as the speed increases. Hence, the rotor position information is an essential part of SRM control. Usually, optical encoders or resolvers mounted on the motor shaft are used to provide the rotor position information. Although these external mechanical position sensors provide the rotor position information with high resolution, they are expensive and are not suitable for

high speed operation. Moreover the capability of the accurate positioning of the switching angle is highly dependent upon the performances of the encoder and the microprocessor. That is used to implement high performance control algorithms in most previous studies [2-4]. In particular, as the speed of the SRM increases, the turn-on and turn-off angles fluctuate back and forth from the preset values, which is caused by the resolution of the encoder and the relatively increased sampling period of the microprocessor. Consequently, the higher the speed of the SRM is increased, the larger the amount of the switching angle fluctuations are, and also the more serious the effect of the fluctuations on the SRM drive performance and stability becomes. On the other hand, several works on a sensorless SRM drive have been reported in literature [5-7]. But it suffers from poor resolution at high speed because of the errors caused by the position estimation algorithms and the sampling time of the microprocessor. Therefore, a low cost and simple encoder is proposed in this paper for the practical and high precision SRM drive over a wide speed range along with the control algorithm to provide the switching signals using a simple digital logic circuit.

In this paper, the authors focus on the practical issues by describing technical considerations, design, and implementation for a wide speed range operation of the SRM using an inexpensive 80C196KC microcontroller. The focus here is strictly on the feasibility of implementing an encoder and its controller in a cost-effective manner.

As a result, with variable dc voltage source, a stable wide speed SRM drive capable of bi-directional speed operation has been designed and implemented. In addition, PWM current shaping control can be also applied at low speed range. It is verified from the experiments that the proposed encoder and the logic controller can be a powerful candidate for the practical low cost SRM drive.

## 2. Conventional SRM Drives

Because the SRM is a doubly-salient, singly-excited motor with one or more phases excited at a time, its torque production mechanism is based on reluctance principle. Fig. 1 shows the typical configuration of 8/6 SRM. Because of the double saliency as shown in the

figure, the stator and rotor poles tend to align together to offer minimum reluctance path for the main flux produced by the excited stator phase. Thus, by sequentially exciting the stator phases, a unidirectional torque can be generated and its amount per phase can be written as follows.

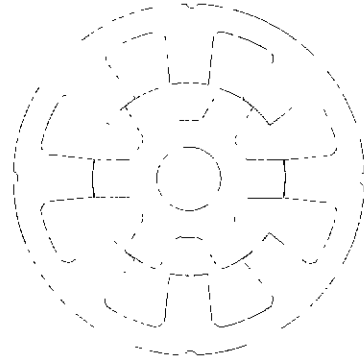


Fig. 1 Configuration of 8/6 SRM

$$T = \frac{1}{2} i^2 \frac{\partial L(\theta, i)}{\partial \theta} \quad (1)$$

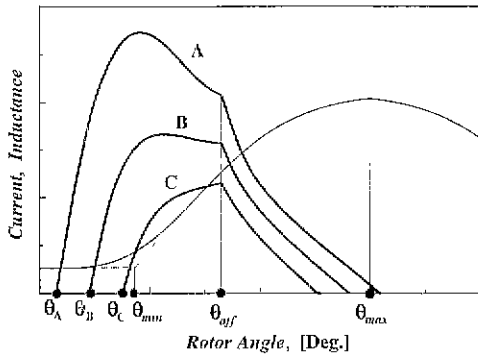
where T denotes the torque, I is the stator current, and L is the inductance.

Therefore, it is important to utilize the torque production interval effectively by energizing and de-energizing the phase currents according to the load torque at the preset turn-on and turn-off angles. If all the four phases are assumed to be symmetrical, the mutual inductance among them can be neglected. A mathematical model of a per phase SRM is given by the equations;

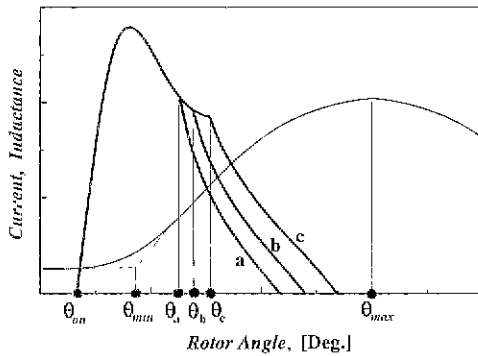
$$V = Ri + L(\theta, i) \frac{di}{dt} + i \frac{dL(\theta, i)}{d\theta} \omega \quad (2)$$

where  $\omega = \frac{d\theta}{dt}$  is angular speed of the rotor [rad/s], R is the resistance of the stator winding.

Fig. 2 shows the unsaturated phase inductance profile and phase current waveforms according to the variation of turn-on and turn-off angles[9].  $\theta_{min}$  and  $\theta_{max}$  in the figure denote the unaligned and aligned position angles between the stator and rotor, respectively.



(a) Variation of the turn-on angle (turn-off angle is fixed)



(b) Variation of the turn-off angle (turn-on angle is fixed)

Fig. 2 Phase current waveforms according to the variation of the turn-on and turn-off angles

If the turn-on angle varies from  $\theta_1$  to  $\theta_C$  with fixed turn-off angle (see Fig. 2(a)), the peak values and hence the durations of the phase currents are different from each other and these values are nearly proportional to the advance angle from  $\theta_{min}$  when the winding resistance is neglected. And if the turn-off angle varies from  $\theta_a$  to  $\theta_c$  with fixed turn-on angle (see Fig. 2(b)), the peak values are the same but the duration intervals are increased. In these turn-on and/or turn-off angle controls, it is essential that the switching angles must be carefully scheduled and controlled to obtain the desired speed and torque. In particular, the phase current should be controlled to reach the zero value before  $\theta_{max}$  because it generates the negative torque, which is the origin of the torque pulsation and reduction in the mechanical output power.

With these operational principles, a typical conventional SRM drive system can be implemented and

controlled as shown in Fig 3. The whole system is consisted of controller, PWM inverter, current and position sensors, and SRM. The controller includes the current controller, speed controller, and speed estimator. The speed controller, generates the reference torque signal by comparing the estimated speed with the reference speed, and then produces the reference current that can produce the desired torque from the lookup table using the reference torque and the rotor position angle  $\theta$ . Each phase current controller forces the motor phase currents to track the references.

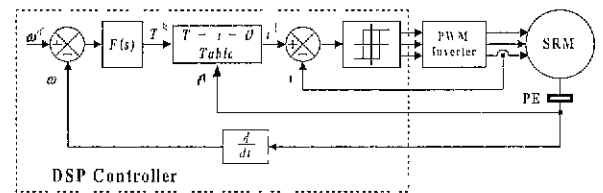


Fig 3 Block diagram of the conventional SRM drive system

In this conventional SRM drive system, mechanical position sensors generate a finite number of pulses per revolution and its maximum decides the position resolution. If the number of pulses per revolution is  $n_p$ , the mechanical position resolution of the encoder,  $\Delta\theta_e$ , can be given as follows,

$$\Delta\theta_e = \frac{360}{n_p} \text{ [deg.]} \quad (3)$$

In addition, the microprocessor also puts a limitation on the accuracy of the motor position because it takes a nonzero time interval to estimate the angle and generate the switching signals. The time required for the microprocessor is called control action cycle in this paper. If the control action cycle is  $T_s$ , then the error in the angle  $\Delta\theta_m$  is given by

$$\Delta\theta_m = \omega \cdot T_s \cdot \frac{180}{\pi} \text{ [deg]} \quad (4)$$

The sum of these two factors is the maximum switching angle error of the conventional SRM drive system and given as

$$\Delta\theta_s = \Delta\theta_e + \Delta\theta_m = \frac{360}{n_p} + \omega \cdot T_s \cdot \frac{180}{\pi} \text{ [deg.]} \quad (5)$$

The relation between the switching angle error and rotor speed can be plotted as Fig. 4.

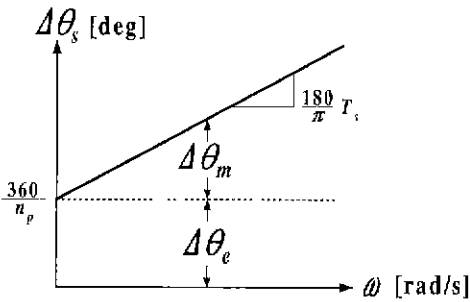


Fig. 4 Switching angle deviations according to the speed variation

From the above equation, even though the estimation of the rotor position angle is successfully performed, the errors between the estimated and real switching angles always exist. In general, when the motor speed is low, the accuracy of the switching angle is mainly dependent upon the resolution of the encoder, because the fluctuation of turn-on and turn-off angle by the sampling period is much less than that of the resolution of the encoder. However, if the motor operates in a higher speed region, then the accuracy of the switching angle is mainly dependent upon the sampling period of the microprocessor.

### 3. Proposed Encoder and Logic Controller

The proposed control system incorporates a dedicated hardware digital angle controller which receives the angle commands from the feedback loop and translates them into transistor conduction angles which are synchronized to the rotor position. The basic control parameters of the drive system can be summarized as follows:

- $I$  chopping current level(current control mode), which is also the peak-limiting current in the constant power region(single pulse mode).
- $V_{dc}$  DC input voltage level in the constant torque region(voltage control mode).
- $\theta_{on}$  turn-on angle
- $\theta_{off}$  turn-off angle.

#### Proposed Encoder

As mentioned earlier, to achieve a wide speed range operation of the SRM with the precise angle control, it is essential to design a SRM drive system that can maintain

its accurate performance irrespective of the resolutions of the encoder and the microprocessor speed. In addition, for practical industrial and residential applications, the cost reduction and compact size of system are also required. Therefore, a novel, but simple encoder and associated digital logic control algorithm are presented in this section and are shown in Fig. 5 and 6. The proposed encoder disk in Fig. 5 is designed for 8/6 SRM and has two tracks of the slits, FW(forward) and BW(backward). In 8/6 SRM, the period of the phase inductance profile,  $\beta$ , can be generally written as follows.

$$\beta = \frac{360}{P_r} \text{ [deg.]} \tag{6}$$

Where  $P_r$  is the number of poles of the rotor. The phase turn-on interval is also determined according to the number of poles of stator and rotor.

$$\delta = 2 \cdot \frac{360}{P_s \cdot P_r} \text{ [deg.]} \tag{7}$$

Where  $P_s$  is the number of poles of the stator.

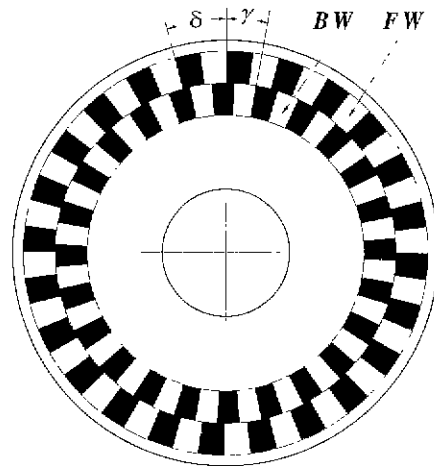


Fig. 5 Double-track encoder

For the 8/6 SRM,  $\beta$  and  $\delta$  are  $60^\circ$  and  $15^\circ$ , respectively. Therefore, to determine the phase turn-on and turn-off angles, a rising edge of the incoming phase is required in every switching period which will be the turn-off angle of the outgoing phase. Therefore, the angle width of the proposed encoder slit is chosen to be  $7.5^\circ$ . In the case of 6/4 SRM, that will be  $15^\circ$ .

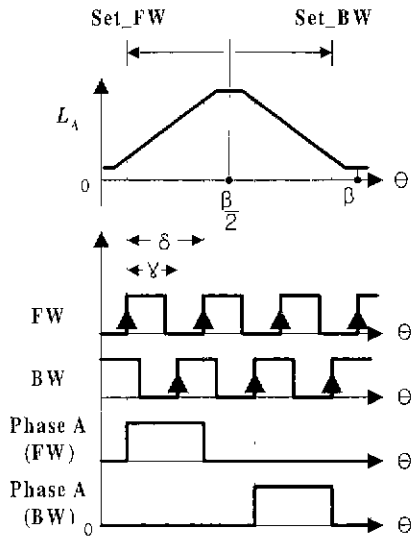


Fig. 6 Switching patterns of the phase switch for forward and backward rotations

The FW and BW slit arrays, which are used to rotate the motor in forward and backward directions, respectively, consist of 24 slits and have an angle difference of  $\gamma$ . When the motor is rotating in the backward direction, the current pulse has to be established where the inductance profile has a negative slope. Hence,  $\gamma$  is a turn-on angle difference between the forward and backward rotation. In this paper,  $\gamma$  is chosen as  $10^\circ$ . Using the encoder disk and two optical sensors, the pulse signals can be generated to determine the phase switching angle. The basic algorithm of the switching pattern generation is illustrated in detail in Fig 6. The figure shows the motor inductance profile, FW and BW signals, gate signals for forward and backward rotation and their relationship. When the motor rotates in a forward direction, the turn-on and turn-off angles of the phase windings are determined by the rising edges of FW pulse signals. In this case, a Set\_FW is the reference position and the phase A turn-on angle can be determined at every 4 counter period of the FW signals from the Set\_FW. The gate signals of the B-D phases are obtained by mutually shifting the phase A signal by  $15^\circ$  using a ring counter. When the motor rotates backwards, a Set\_BW is the reference position and the logic algorithm is identical. The decision of the forward and backward rotation of the motor can be made using FW and BW pulses by the same method in the conventional

incremental encoder. Since a phase switching angle is directly obtained from the encoder via a simple correction process by the digital logic controller, the position and interval of the phase switching angle is always identical and the precise angle control can be achieved.

### Digital Logic Controller

Fig. 7 shows the phase inductance profiles, encoder output signals and gate signals of the proposed system. Note that to describe the generation of the switching patterns more clearly, the position angle axis of the BW signals and phase gate signals are inverted in the figure. Each phase switch should be set to ON at every 4th rising edge of the FW pulses of the encoder for the forward rotation. For this purpose, 4 bit counter and 2/4 multiplexer that need 2 control line are adopted instead of 4 bit register that needs 4 control line. In a similar way, each phase switch is set to ON at every 4th rising edge of the BW pulses for the backward rotation.

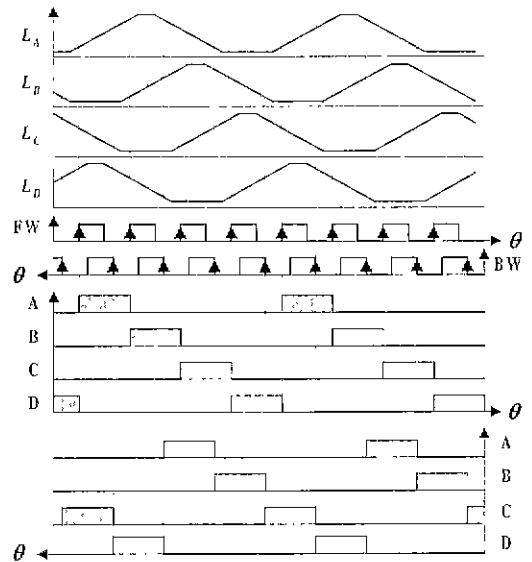


Fig. 7 Gate signals for each phase switch when SRM is rotating in the forward and backward directions by the proposed encoder

The proposed control method has a limitation of the fixed turn-on and turn-off angles over the whole speed range. Therefore, to change the motor speed appropriately, the current level control by the delta modulation technique or the motor input voltage control

should be adopted. Fig. 8 shows the SRM, its power circuit, and buck converter. In the figure, subscripts  $A$ ,  $U$ , and  $D$  of the SRM and power circuit correspond to the phase, up and down, respectively.  $V_{dc}$  and  $V_c$  denote the motor input voltage and the source voltage, respectively. The motor input voltage is controlled by the buck converter. With this configuration, both methods can be adopted.

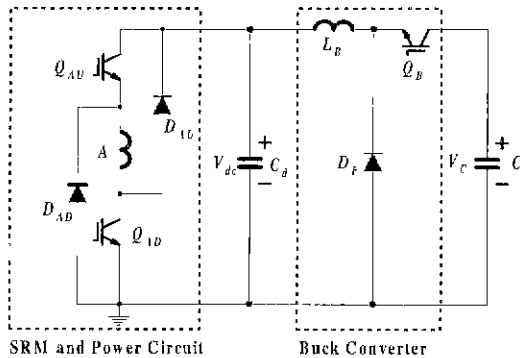


Fig. 8 Schematic diagram of SRM drive system

Fig. 9 shows the block diagram of the proposed logic controller of SRM drive system to generate the gate signal. The controller is implemented using 80C196KC for the practical application. The operation of the controller can be illustrated as follows; First, for starting, the rotor of the motor is forced to be placed at initial position  $\theta_0$  (see Fig. 7) by switching on  $Q_{CU}$  and  $Q_{CD}$  by enabling the terminal  $L$ (load) of the counter and using the 2/4 multiplexer. In this position, phase  $A$  switches,  $Q_{AU}$  and  $Q_{AD}$ , should be set to ON by selecting the FW signals at the DIR terminals for the forward rotation of the motor, or phase  $B$  switches,  $Q_{BU}$  and  $Q_{BD}$ , should be set to ON by selecting the BW signals for the backward rotation. And to monitor whether the switching sequence under the starting and running operations is correct or not, the upper 4 bits of the port 0 are always checked. If the fault in the switching sequence occurs, it will be corrected via port 0. The decision of the rotational direction is made by detecting the phase angles of the FW and BW signals that are input to the high speed input (HSI) terminals. Using the FW or BW signals that are input to the timer 2 of the 80C196KC, the motor speed is evaluated by the M/T method [8].

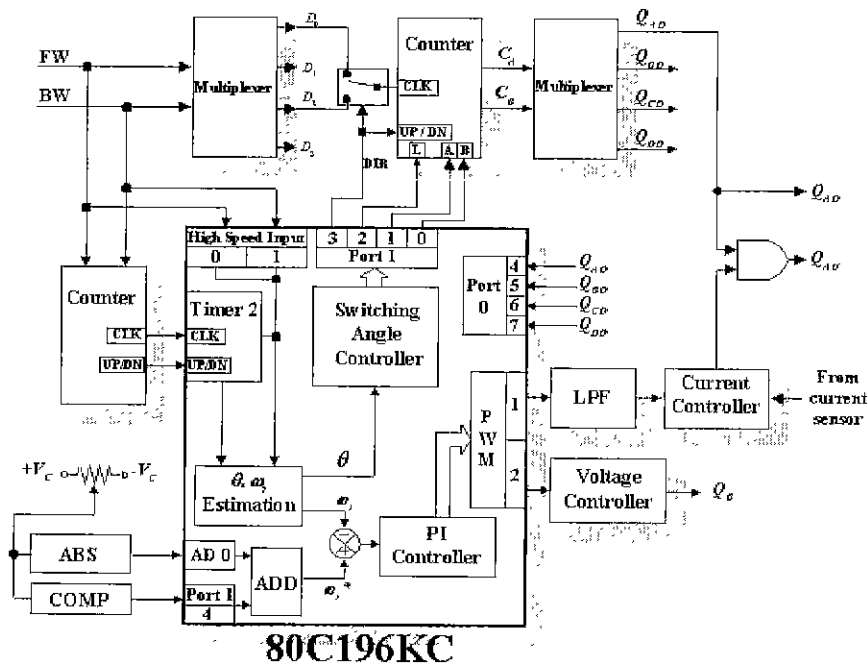
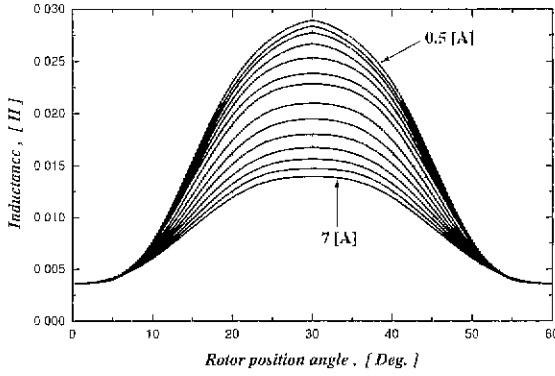


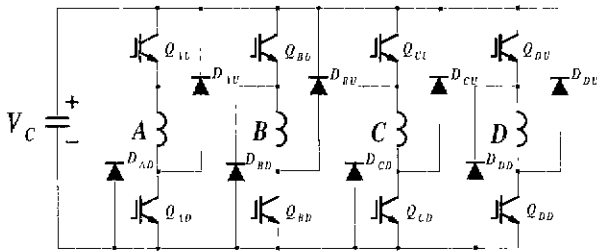
Fig. 9. Block diagram of the proposed 80C196KC-based logic controller of SRM drive system

### 4. Experimental Results

The experiments are performed using a 8/6, 400 W, 160 V SRM. Its inductance profile measured at every 0.5-A step according to the one mechanical angle step is shown in Fig. 10(a). Phase resistance  $R_{ph}$  is 2.0  $\Omega$ , unaligned phase inductance  $L_u$  is 29 mH, aligned phase inductance  $L_a$  is 37 mH. To excite the motor windings, a conventional classic inverter as shown in Fig. 10 (b) is used.



(a) Measured inductance profiles of SRM



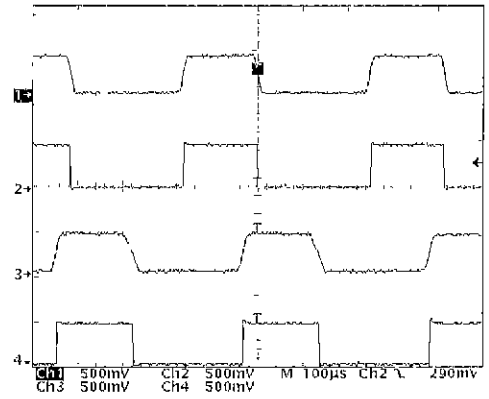
(b) Classic inverter circuit for SRM drive

Fig. 10 The inductance profiles and structure of SRM

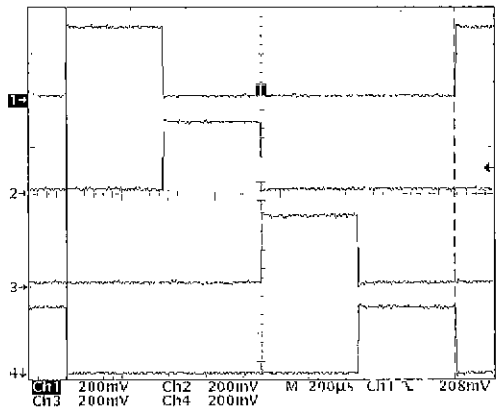
The experiments are performed at the conditions that the turn-on angle is set to 10° and turn-off angle is set to 25°, and the motor speeds are 1,800 and 6,000 rpm with the load torque of 1.2 and 0.4 Nm, respectively.

Fig. 11 shows the experimental results of SRM drive system using the proposed encoder when the motor is rotating at 6000 rpm. Fig. 11(a) shows the phototransistor output signals (first and third) by BW and FW slit arrays, and their hysteresis comparator output signals (second and fourth). It can be shown that the comparator output signals have an uniform time interval

cycle by cycle. It means that the pulse rising edges, hence the phase gate signals are switched on precisely at the preset position. Note that since only the uniformity of the pulse rising edge has the meaning, the discrepancy between the ON and OFF intervals of the signals, which is caused by the light diffraction, is not important. Fig. 11(b) shows the gate signals of each phase. In the figure, B-D phase pulses (from the second to the fourth) is obtained by mutually shifting the phase A pulse by 15°. It can be also shown that each phase gate signal has an identical turn-on interval. The measured phase current waveforms have the same peak value and hence the same waveshape cycle by cycle as shown in Fig. 11(c). It means that the phase switches are accurately turned on and off at the preset position angle for every cycle.



(a) Output signals of photo transistor and encoder



(b) Phase gate signal

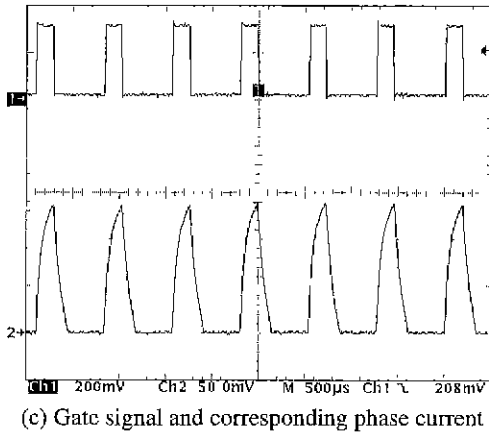


Fig. 11. Waveforms of the gate signals and phase currents (6,000 rpm)

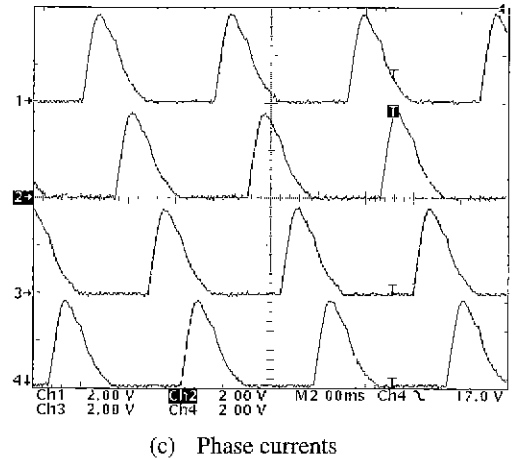


Fig. 12 Waveforms of the gate signals and phase currents (1,800 rpm)

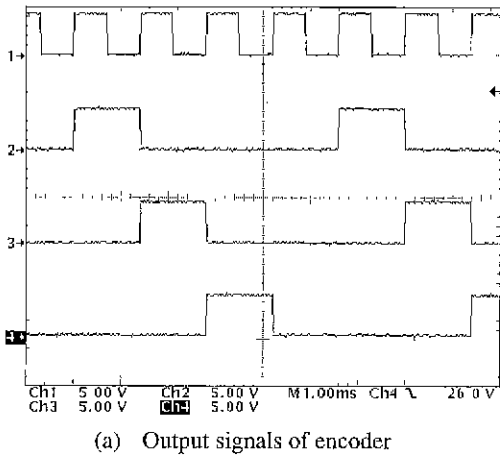
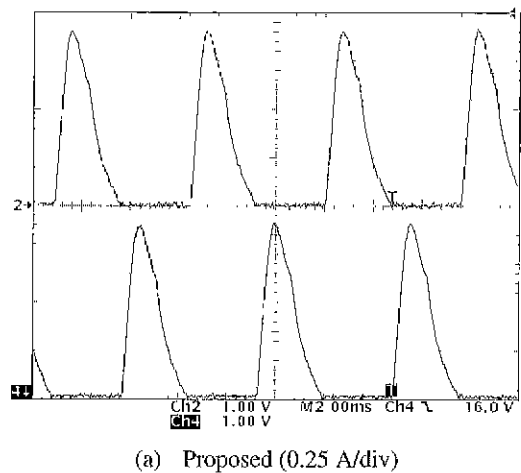
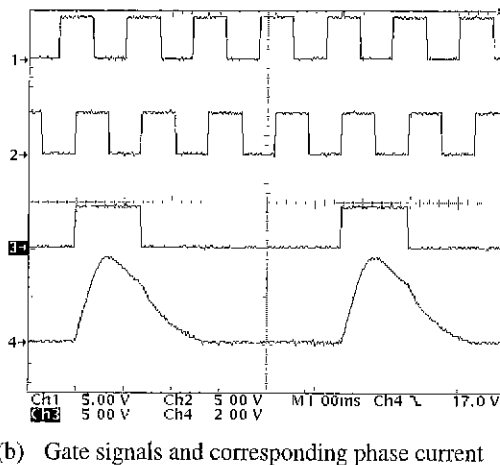
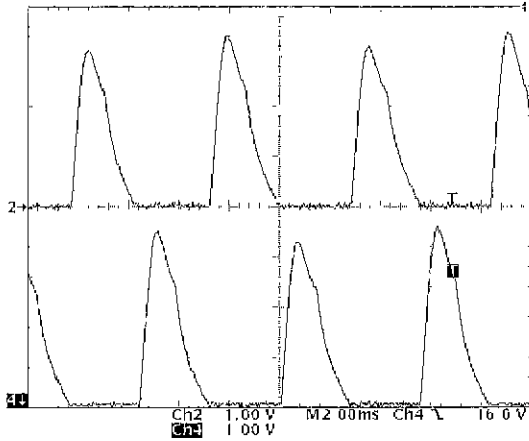


Fig. 12 that shows the comparator output pulses, the phase gate signals, and the phase current waveforms when the motor speed and torque are 1,800 rpm and 1.2 Nm, respectively. It can be shown that the desirable feature of the proposed control system is maintained identically from Fig 12(c), in which each phase current has the same peak value and waveform.

Fig 13 is presented to demonstrate the effectiveness of the proposed system by comparing it with the conventional one in Fig. 3. The conventional system is implemented using 500 pulse per revolution incremental encoder and TMS320C40 high speed floating-point DSP are driven with the same operating conditions of 1,800 rpm and 1.2 Nm.







(b) Conventional (0.25 A/div)

Fig. 13 Comparison of phase current waveforms (1,800 rpm).

While the current pulses have the same shape for the proposed one (Fig. 13(a)), as shown in the Fig. 13(b), the conventional drive shows fluctuating peak value. In the conventional system, if the motor speed is increased, it is much clearer from the Fig. 13(b) that the switching angles are perturbed back and forth and the current waveforms are also much different from every cycle and phase. This is due to the resolution of the encoder and the sampling period of the DSP controller, as mentioned earlier. Because this switching angle deviation can cause the torque pulsation, the drive system can be unstable in the high speed region.

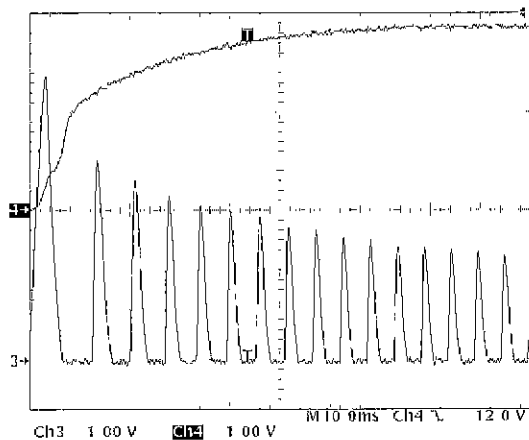
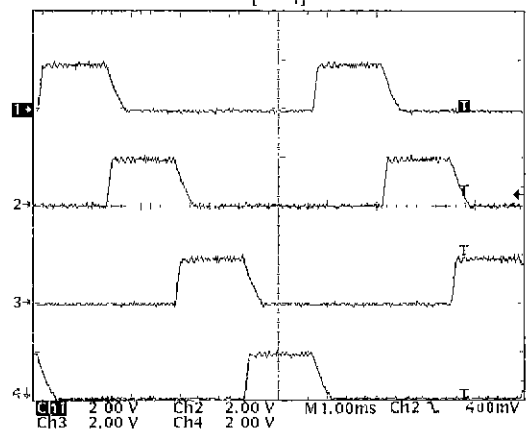


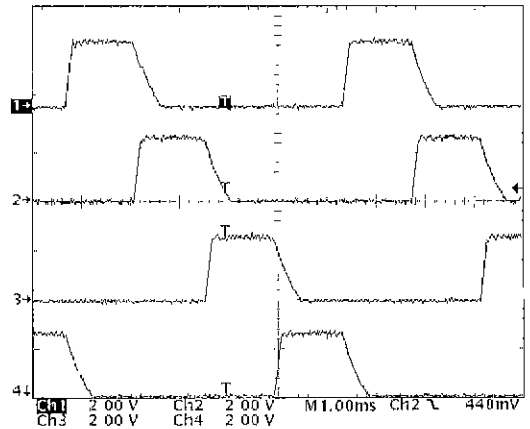
Fig. 14 Speed and current waveforms at starting by variable DC voltage

Fig 14 shows the experimental results of the no-load

start-up operation by the voltage control method in the proposed system. The upper and lower traces are the speed and current waveforms, respectively.



(a)  $T_L = 1 \text{ Nm}$  (2 A/div)



(b)  $T_L = 2 \text{ Nm}$  (2 A/div)

Fig. 15 Phase current waveforms with load variation (1,800 rpm)

Fig 15 shows the experimental results of the current level control when the speed is constant at 1,800 rpm and load torques are 1 and 2 Nm. In these cases, the phase switches are also turned on and off accurately at the preset position angle for every cycle and phase. Therefore, the proposed system can be a practical and stable alternative for wide speed SRM drive not only because it can control the switching angle accurately but also because it can be implemented by the low cost encoder and the simple digital logic controller.

## 5. Conclusions

Generally, SRM drive system should have the capability of the accurate switching on the preset turn-on and turn-off angles in order to obtain a stable operation in a wide speed range. The accuracy of the switching angles is dependent upon the resolution of the encoder and the sampling period of the microprocessor in the conventional system. IN order to circumvent the limitations on the accuracy, the low cost encoder suitable for the practical and stable SRM drive is proposed and the control algorithm to provide the switching signals using the simple digital logic circuit is also presented in this paper. As a result, a stable wide speed SRM drive can be achieved by the proposed high precision angle control. It is verified from the experiments that the proposed encoder and logic controller can be a powerful candidate for the practical low cost SRM drive.

## References

1. T. J. E. Miller, *Switched Reluctance Motor and Their Control*, Oxford, UK, Clarendon, 1993.
2. I. Husain and M. Ehsani. "Torque Ripple Minimization in Switched Reluctance Motor Drives by PWM Current Control," *IEEE Trans. on Power Electronics*, Vol. 11, No. 1, pp. 91-98, 1996.
3. B. K. Bose, T. J. E. Miller, P. M. Szezesny and W. H. Bocknell, "Microcomputer Control of Switched Reluctance Motor," *IEEE Trans. on Industrial Applications*, Vol. 22, No. 4, pp. 708-715, 1986.
4. P. H. Chappell, W. F. Ray and R. J. Blake, "Microprocessor Control of a Variable Reluctance Motor." *Proc. IEE*, Vol. 131, No. 2, Part. B, pp. 51-60, 1984.
5. B. Y. Ma, W. S. Feng, T. H. Liu and C. G. Chen, "Design and Implementation of a Sensorless Switched Reluctance Drive System." *IEEE Trans. on Aerospace and Electronic Systems*, Vol. 34, No. 4, pp. 1193-1207, 1998.
6. S. R. MacMinn, W. J. Rzesos, P. M. Szezesny and T. M. Jahns, "Application of Sensorless Integration Techniques to Switched Reluctance Motor Drives," *IEEE Trans. on Industrial Applications*, Vol. 28, No. 6, pp. 1339-1344, 1986.
7. M. Ehsani, I. Husain and A. B. Kulkarni, "Elimination of Discrete Position Sensor and Current Sensor in Switched Reluctance Motor Drives," *IEEE Trans. on Industrial Applications*, Vol 28, No. 1, pp. 128-135, 1992.
8. J. Y. Hung and Z. Ding, "Minimization of torque ripple in permanent magnet motors: A closed form solution." in *Conf. Rec. IECON '92*, pp. 459-463, 1992.
9. J. W. Ahn. *Switched Reluctance Motor*, O-Sung Media, 2001.